Finite Element Modeling for the Design of a Single-Screw Extruder for Starch-Based Snack Products

Ram Yamsaengsung* and Chumporn Noomuang

Abstract **—** The design of a single-screw extruder for starch-based snack products was studied using 3-D Finite Element Modeling in Polyflow to simulate the flow of rice flour dough through an extruder. The generalized Newtonian model was used to characterize this material in the initial stages in order to develop an extruder than could properly mix and transport the material to the injection nozzle of the extruder. Using a screw speed of 50 rpm and a constant viscosity of 10,000 Pa s, the size of the motor required for the extruder was about 5.2 hp.

Index Terms **—** Finite Element Modeling, Numerical Simulation, Single-Screw Extruder, Starch Snacks

I. INTRODUCTION

The designing of single- and twin-screw extruders in developing countries have been very limited due to the complexity of the system and the lack of advanced simulation software in the past, However, within the last decade, numerous computational fluid dynamic software have been developed and are applicable to varieties of products from plastic melts to flour based snack products [1]-[3]. Other more typical extruder products include pasta noodles, expanded snacks, cereals, and pie crust dough [4]-[6]. Many different laws such as Newtonian, Power-Law, Herschel-Bulkley Law, Bird-Carreau Law, Bingham Law, Carreau-Yasuda Law, and Cross Law have been developed to describe the flow of these materials and the change in viscosity as a function of shear rate [7]. This particular work deals with the design of a single screw extruder for the processing of starch based snack products using the computational software POLYFLOW 3.12.

II. MATERIALS AND METHODS

A. Single Screw Extruder

Fig. 1 shows a commercial single screw extruder and Fig. 2 depicts the major parts of the extruder including the feed section, the melt section or the metering section, and the die section or the injection section.

Figure 1: A typical commercial single-screw extruder [8].

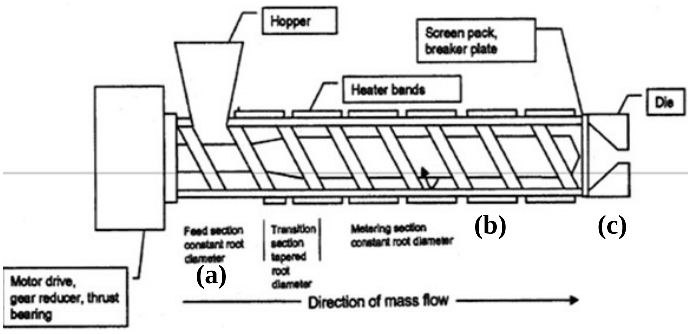

Figure 2: Schematic of a single-screw extruder showing the (a) feed section, (b) the metering section, and (c) the die section or the injection section [9].

B. Simulation of Flow through Extruder

The geometry of the single-screw extruder was created using AutoCAD 2007. Fig. 3 depicts the drawing of the feed section of the extruder, the rotational direction of the screw, and the direction of flow of the material. The flow of the material is indicated by the space between the screw and the wall of the extruder.

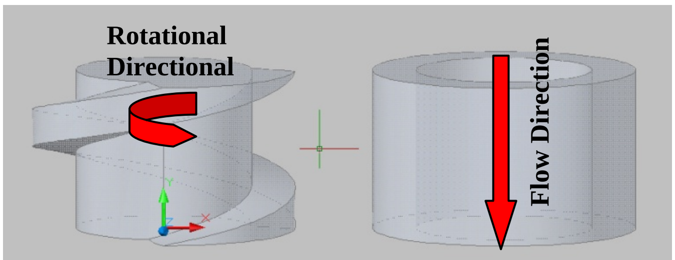

Figure 3: Drawing of feed section of the extruder indicating rotational direction and flow direction for one screw section.

Manuscript submitted on March 18, 2010. This work was supported in part by the Prince of Songkla University.

*R.Yamsaengsung is with the Department of Chemical Engineering, Faculty of Engineering, Prince of Songkla University, Hat Yai, Thailand, 90112 (corresponding author; phone: +6672-287291; fax:+6674-212-896; e-mail: ram.y@psu.ac.th).
C.Noomuang is a PhD student with the Department of Chemical Engineering, Faculty of Engineering, Prince of Songkla University, Hat Yai, Thailand, 90112.

ISBN: 978-988-18210-8-9
ISSN: 2078-0958 (Print); ISSN: 2078-0966 (Online)

Once the AutoCAD drawing has been created, the meshing of the elements for the simulation process was conducted using GAMBIT 2.4.6. Hexagonal volume elements were used to represent 3-D modeling. The boundary regions for the volume elements were included (1) Inflow1 (origin of flow), Outflow2 (exit of flow), Wall3 (surface of screw), and Wall4 (inner surface of extruder). Next, the volume elements of the region between the boundary surfaces were assigned as Fluid1 which corresponds to the area of simulation, while the screw and wall area were assigned as Solid2 indicating stationary solid plane. Finally, the quality of the mesh was analyzed using the command Examine Mesh. If the value of the examination approached 0, the quality is deemed acceptable. Fig. 4 shows the meshing of the volumetric elements.

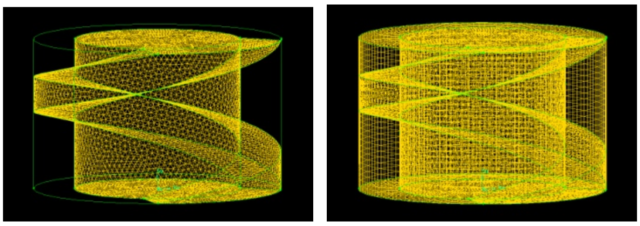

Figure 4: Meshing of elements for the simulation of flow.

Once the volume elements have been created, the file was exported as Generic Neutral (.neu) type and converted into POLYFLOW format mesh file using ANSYS POLYFLOW 3.12.2. In the POLYDATA section of ANSYS, a New Task was created and set as an F.E.M. (Finite Element Method) task and as a steady-state problem. In the Sub-Task box, the Generalized Newtonian Isothermal Flow Problem was selected and a Domain of the Sub-Task and the Sub-Domain were created. In the Material Data box, the choice of Shear-Rate Dependence of Viscosity included Constant Viscosity, Bird-Carreau Law, Power Law, Bingham Law, Herschel-Bulkley Law, Cross Law, Log-Log Law, Modified Bingham Law, Modified Herschel-Bulkley Law, Carreau-Yasuda Law and Modified Cross-Law. In this preliminary study, the value was set to Constant Viscosity indicating a Newtonian type fluid. Finally, the Flow Boundary Conditions were assigned as Inflow with a given flow rate and as Outflow which is acted upon by an Imposed Velocity. The results of the simulation were displayed using CFD-Post 12.0.1.

In this study, three different sections of the extruder were investigated: (1) the feed section, (2) the metering section, and (3) the die section. All three sections were drawn, meshed, and simulated separately to demonstrate the flow of material in each region.

C. Governing Equations

For a generalized Newtonian flow, POLYFLOW solves the momentum equations, the incompressibility equation, and (for non-isothermal flows) the energy equation [7]. The form of the momentum equations is

$$-\nabla p + \nabla \cdot T + f = \rho a \qquad (1)$$

where p is pressure, T is extra-stress tensor, f is volume force, ρ is density, and a is acceleration. The incompressibility equation is

$$\nabla \cdot v = 0 \qquad (2)$$

where v is velocity. The energy equation is presented as Equation (3) below.

$$\rho C_p \frac{DT}{Dt} = r - \nabla \cdot q + (\sigma D) \qquad (3)$$

where σ is the Cauchy stress tensor, D is the rate-of-deformation tensor and (σD) is the sum of the diagonal terms of σD (i.e., the trace operator).
DT/Dt is the material derivative of the temperature:

$$\frac{DT}{Dt} = T : \nabla v + r - \nabla \cdot q \qquad (4)$$

For a generalized Newtonian fluid,

$$T = 2\eta D \qquad (5)$$

where D is the rate-of-deformation tensor and η can be a function of local shear rate $\dot{\gamma}$, temperature T, or both. The local shear rate is defined as

$$\dot{\gamma} = \sqrt{2(D)^2} \qquad (6)$$

In a simple shear flow, $\dot{\gamma}$ reduces to the velocity gradient.
When non-isothermal flow is modeled, POLYFLOW calculates the temperature, velocity, and pressure fields simultaneously (i.e., fully coupled, unless otherwise specified by a change in the default numerical parameters).

D. Input Parameters

To account for Newtonian flow, a constant velocity value of 10,000 Pa·s was used. This approximate value for the rice flour dough corresponded to the one used by Dhanasakharan and Kokini [2] for the extrusion of wheat dough across a single-screw extruder. Moreover, the speed of the screw was set to 50 rpm or 5.236 rad/s.

III. Results and Discussion

Figs. 5-6 show the results of the simulation for the feed section for the velocity profile, the shear rate profile and the pressure gradient. From Fig. 5, the maximum velocity of the material (about 8 cm/s) is highest near the screw surface and smallest near the barrel wall (no slippage, zero velocity boundary condition). This corresponds to the rate of shear where the high shear rate at the wall results in zero velocity at the wall surface as shown in Fig. 6.

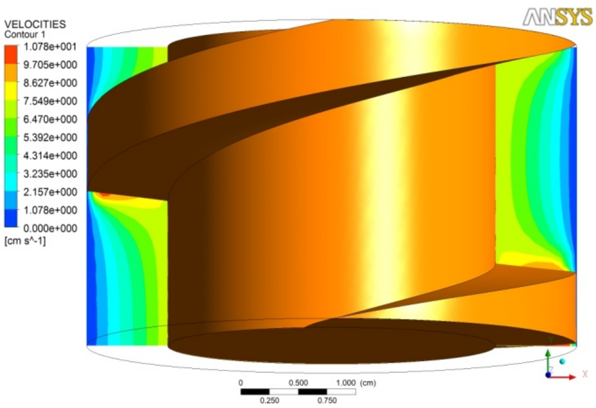

Figure 5: Velocity distribution inside the feed section.

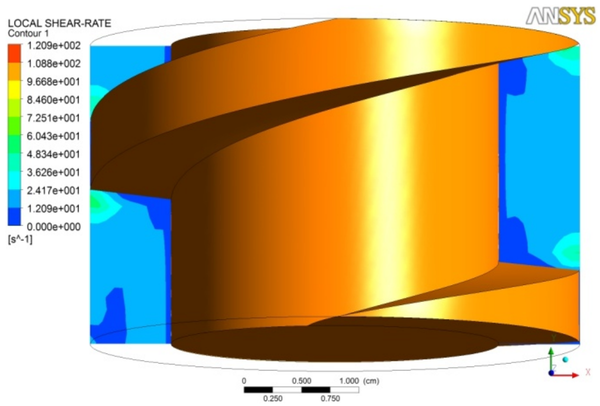

Figure 6: Local shear rate inside the feed section.

For the meter section, the results are shown in Figs. 7-8. In this region, there has been continuous mixing of the flour and water (signified by the rotation of the screw) and the velocity distribution in the axial direction is much more uniform than that in Fig. 5. Likewise, the local shear rate is nearly constant throughout the entire section with exception of the barrel wall. This shows good mixing of the product within the screw barrel indicating steady flow of the product toward the exiting point.

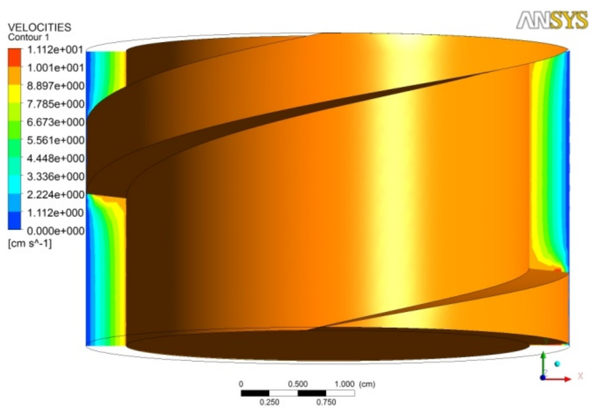

Figure 7: Velocity distribution inside the metering section.

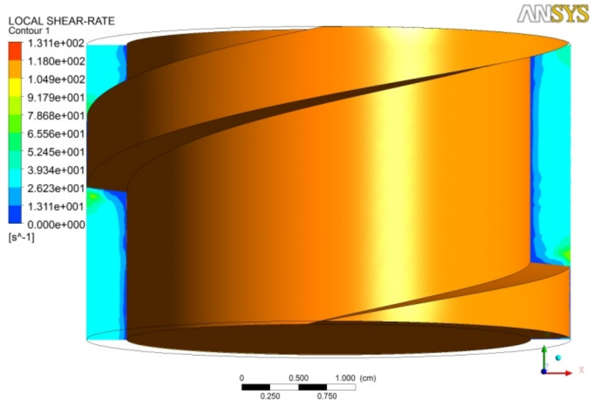

Figure 8: Local shear rate distribution inside the metering section.

Finally, in the injection section, the velocity and local shear rate distribution are shown in Figs. 9-10. The velocity in this region increased to more than 26 cm/s compared to 8-10 cm/s in the feed and metering section. Moreover, the shear rate in the injection region of the screw also increased dramatically from 5 s^{-1} in the metering section to more than 8 s^{-1} in the injection section. The gain in velocity is ideal for the expansion of snack product after it has been injected.

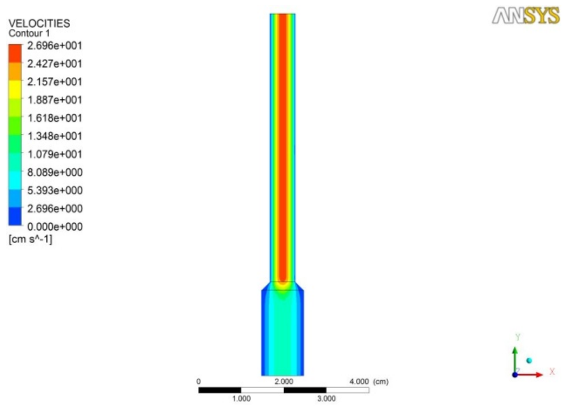

Figure 9: Velocity distribution inside the injection section.

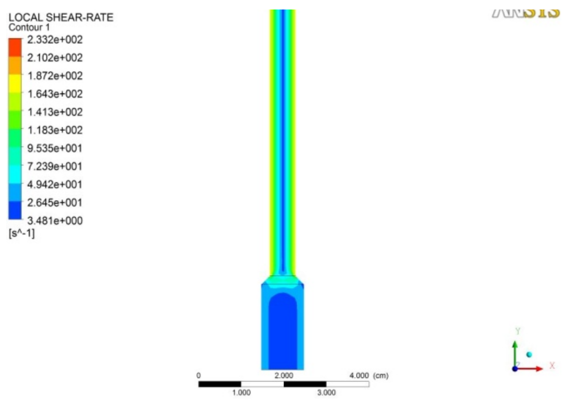

Figure 10: Local shear rate inside the injection section.

From the results of the local shear rate of the material inside the screw, the power of the motor required to operate the screw was determined. In this study, for a material with a viscosity of 10,000 Pa·s and a single-screw extruder speed of

ISBN: 978-988-18210-8-9
ISSN: 2078-0958 (Print); ISSN: 2078-0966 (Online)

50 rpm, the shear rate was approximated to be a 3.934 s^{-1} in the metering section, the required motor power was approximately 5.2 hp.

IV. Conclusion

Hence, by modeling the flow of material inside the extruder, the behavior of the material with shear rate and shearing time can be obtained. More research will have to be conducted to bring about the effect of varying the shear rate and the viscosity of the fluid on the shear stress development inside the screw extruder. This will help shed some light into the proper design of extrusion equipment for complicated food product. In addition, the development of a viscoelastic model for rice flour-based or wheat-based snacks products is essential to fully predict the flow of these types of materials to a single-screw extruder.

Acknowledgment

The team of researcher would like to thank the Prince of Songkla University for the generous financial support in this research. We would also like to thank the Faculty of Engineering and the Department of Chemical Engineering for providing the necessary equipment and facilities to conduct this research.

Reference

[1] Das, M.K., Ghoshdastidar, P.S. 2001. Experimental validation of a quasi three-dimensional conjugate heat transfer model for the metering section of a single-screw plasticating extruder. Material Processing Technology, 120: 397-411.
[2] Dhanasakharan K.M. and Kokini, J.L. 2003. Design and scaling of wheat dough extrusion by numerical simulation of flow and heat transfer. Journal of Food Engineering, 60:421-430.
[3] Lertsiriyothin, W. and Kumtib, M. 2004. Simulation of flour flow in extrusion process by using computational fluid dynamics commercial software. ANCSE-8, July 21-23, 2004, Suranaree University of Technology, Thailand.
[4] Harper, J.M. 1981. Extruder of food (1st ed.). CRC Press. United States of America.
[5] Rauwendaal, C. 2001. Polymer extrusion (4th ed.). New York: Hanser.
[6] White, J.L. 1991. Twin screw extrusion: Technology and principle. New York: Carl Hanser.
[7] Polyflow 3.12 User's Guide . 2008. ANSYS Inc., United States of America.
[8] Accessed from http://www.chinamasterbatch.com/ on March 18, 2010. SA Masterbatch Co. Ltd., China, a manufacturing company of masterbatch, fillers, plastic pellets, injection molding equipment, and extruders.
[9] Accessed from http://www.aapspharmscitech.org on March 18, 2010. The website is an online pharmaceutical science and technology journal with information on drug manufacturing equipment such as extruders.